Identification and Characterization of a Novel and Specific Inhibitor of the Ataxia-Telangiectasia Mutated Kinase ATM

Ian Hickson,[1] Yan Zhao,[2] Caroline J. Richardson,[1] Sharon J. Green,[1] Niall M. B. Martin,[1] Alisdair I. Orr,[1] Philip M. Reaper,[3] Stephen P. Jackson,[3] Nicola J. Curtin,[2] and Graeme C. M. Smith[1]

[1]KuDOS Pharmaceuticals Ltd., Cambridge Science Park, Milton Road, Cambridge; [2]Northern Institute for Cancer Research, Medical School, University of Newcastle upon Tyne, Newcastle upon Tyne; and [3]Wellcome Trust and Cancer Research UK Gurdon Institute and Department of Zoology, Cambridge University, Cambridge, United Kingdom

ABSTRACT

The serine/threonine protein kinase ATM signals to cell cycle and DNA repair components by phosphorylating downstream targets such as p53, CHK2, NBS1, and BRCA1. Mutation of *ATM* occurs in the human autosomal recessive disorder ataxia-telangiectasia, which is characterized by hypersensitivity to ionizing radiation and a failure of cells to arrest the cell cycle after the induction of DNA double-strand breaks. It has thus been proposed that ATM inhibition would cause cellular radio- and chemosensitization. Through screening a small molecule compound library developed for the phosphatidylinositol 3′-kinase–like kinase family, we identified an ATP-competitive inhibitor, 2-morpholin-4-yl-6-thianthren-1-yl-pyran-4-one (KU-55933), that inhibits ATM with an IC_{50} of 13 nmol/L and a Ki of 2.2 nmol/L. KU-55933 shows specificity with respect to inhibition of other phosphatidylinositol 3′-kinase–like kinases. Cellular inhibition of ATM by KU-55933 was demonstrated by the ablation of ionizing radiation-dependent phosphorylation of a range of ATM targets, including p53, γH2AX, NBS1, and SMC1. KU-55933 did not show inhibition of UV light DNA damage induced cellular phosphorylation events. Exposure of cells to KU-55933 resulted in a significant sensitization to the cytotoxic effects of ionizing radiation and to the DNA double-strand break-inducing chemotherapeutic agents, etoposide, doxorubicin, and camptothecin. Inhibition of ATM by KU-55933 also caused a loss of ionizing radiation-induced cell cycle arrest. By contrast, KU-55933 did not potentiate the cytotoxic effects of ionizing radiation on ataxia-telangiectasia cells, nor did it affect their cell cycle profile after DNA damage. We conclude that KU-55933 is a novel, specific, and potent inhibitor of the ATM kinase.

INTRODUCTION

The cellular response to DNA damage is one of coordinated repair and moderation of proliferation (1). ATM is a protein kinase member of the phosphatidylinositol 3′-kinase (PI3K)–related kinase (PIKK) family (2) that plays a critical role in the maintenance of genome integrity (3, 4). The M_r 345 000 phospho-protein plays key roles in coordinating cellular responses to IR-induced DNA double-strand breaks. Mutation of *ATM* occurs in the human autosomal recessive disorder ataxia-telangiectasia (A-T), which is characterized by several symptoms, including cerebellar degeneration, oculocutaneous telangiectasia, growth retardation, immune deficiencies, and characteristics of premature aging (5, 6). At the cellular level, A-T is characterized by a hypersensitivity to ionizing radiation and radiomimetic drugs, radioresistant DNA synthesis, and chromosomal instability (5, 6). In addition, there is a failure of A-T cells to arrest the cell cycle after DNA damage, thus reducing the opportunity for the repair of the genome before DNA replication or mitosis (6). Exposure of normal cells to ionizing radiation results in cell cycle arrest and ATM appears to be critical for the induction of these events, orchestrating the response by the downstream signaling to other response factors (3, 4, 7–9). Substrates or phosphorylation target sites for ATM have been implicated at the level of the G_1 (*e.g.,* p53, Chk2, and Mdm2; refs. 10–13), S phase (*e.g.,* Chk2 and NBS1; refs. 12, 14) and G_2 (*e.g.,* hRAD17 and Brca1; refs. 15, 16) checkpoints.

The increased sensitivity of A-T cells to ionizing radiation is not associated with defective repair of DNA single-strand breaks or in the removal of base damage from DNA (17, 18). Instead, after exposure to ionizing radiation, A-T cells have been reported to display residual chromosomal breaks (19), slower DNA DSB rejoining than wild-type cells (20), and a failure to repair all DNA DSBs (21), which could account for the radiosensitivity and genome instability associated with A-T (5). In light of these findings, it has been proposed that inhibition of ATM may give rise to radiosensitization and that ATM therefore represents an attractive target for the development of new radiosensitizing agents (*e.g.,* ref. 22).

To date, studies designed to test the effects of ATM inhibition on radiosensitivity have mainly used the relatively nonspecific PIKK and PI3k inhibitors wortmannin and caffeine (*e.g.,* ref. 23). Although the ATM-directed p53 response has been shown to be diminished in these experiments, it is most likely that the increased sensitivity to ionizing radiation observed was manifested through the ability of wortmannin and caffeine to inhibit not only ATM but a number of PIKKs, including ataxia-telangiectasia and Rad3-related kinase (ATR), the DNA-dependent protein kinase (DNA-PK), as well as PI3K (*e.g.,* refs. 23–28). These small molecule approaches have demonstrated the feasibility of achieving sensitization to ionizing radiation but have not proven that such sensitization could be achieved by inhibition of ATM alone. Furthermore, wortmannin probably hits too many targets to be a viable clinical agent for the sensitization of tumors to ionizing radiation because the drug covalently modifies large numbers of proteins and is consequently unlikely to be tolerated *in vivo* at radiosensitizing concentrations. In the case of caffeine, the sensitization is by the nonspecific targeting of ATM, ATR, and DNA-PK and the effective concentration is clinically prohibitive. Indeed, serum concentrations of 1 mmol/L, which are required to achieve radiosensitization, are associated with fatal tachyarrythmias (22).

By screening a combinatorial library based around the nonspecific PI3K and DNA-PK inhibitor LY294002 (24, 28), we have identified a novel, specific and very potent small molecule inhibitor of ATM, 2-morpholin-4-yl-6-thianthren-1-yl-pyran-4-one, termed KU-55933. In this article, we describe the characterization of KU-55933 by biochemical means and demonstrate the biological effects of KU-55933 in cell culture model systems to determine the function and specificity of the molecule. Our data not only provide characterization of a novel compound that acts as a radio- and chemosensitizor but also describe a molecular tool that can be used to study the many signaling facets of ATM in the cellular responses to DNA damage. The data also provide a starting point for the development of more potent and pharmaceutically acceptable ATM inhibitors that may ultimately be put to use in clinical settings.

9152

MATERIALS AND METHODS

Chemicals. The compounds, 2-morpholin-4-yl-6-thianthren-1-yl-pyran-4-one (KU-55933) and 2-piperidin-1-yl-6-thianthren-1-yl-pyran-4-one (KU-58050) were synthesized in-house (details to be described elsewhere but see patent WO03070726 for details) and prepared as 10 mmol/L stock solutions in DMSO. For cell-based work, compounds were diluted to give a final DMSO concentration of 0.1 or 0.5%. The chemotherapeutic reagents doxorubicin (Adriamycin), etoposide, melphalan, chlorambucil [Alexis Corporation (United Kingdom) Ltd., Nottingham, United Kingdom], camptothecin, and amsacrine (Sigma, Poole, United Kingdom) were prepared as 5 mg/mL stock solutions in DMSO. Cisplatin [Alexis Corporation (United Kingdom) Ltd.] was prepared as a 1 mg/mL stock in water and mitomycin C [Alexis Corporation (United Kingdom) Ltd.] as a 1 mg/mL stock in methanol. All compounds were diluted in reaction buffer or medium before use in reactions, and in all cases, the concentration of DMSO or methanol was normalized for each drug concentration (in the absence of drug, vehicle control of the appropriate concentration of DMSO, or methanol alone was always used).

Cell Lines and Culture. The human tumor cell lines U2OS, LoVo, SW620, and HeLa B, the A-T fibroblast cell line AT4, and the normal human fibroblast 1BR were cultured as monolayers in DMEM (supplemented with 10% v/v FCS, 100 units/mL penicillin, and 100 μg/mL streptomycin). Glutamine was added to a final concentration of 2 mmol/L. The Chinese hamster cell lines V3 and V3YAC (a kind gift from Penny Jeggo, University of Sussex, Brighton, United Kingdom; ref. 29) were grown in RPMI 1640 containing glutamine (Sigma) and 10% FCS (Sigma). The V3YAC cell line was maintained under Geneticin selection at a final concentration of 500 μg/mL to ensure retention of the YAC.

Purified Enzyme Assays. ATM for use in the *in vitro* assay was obtained from HeLa nuclear extract (Computer Cell Culture Centre, Mons, Belgium) by immunoprecipitation with rabbit polyclonal antiserum raised to the COOH-terminal 400 amino acids of ATM in buffer containing 25 mmol/L HEPES (pH 7.4), 2 mmol/L MgCl$_2$, 250 mmol/L KCl, 500 μmol/L EDTA, 100 μmol/L Na$_3$VO$_4$, 10% v/v glycerol, and 0.1% v/v Igepal. ATM-antibody complexes were isolated from nuclear extract by incubating with protein A-Sepharose beads for 1 hour and then through centrifugation to recover the beads. In the well of a 96-well plate, ATM-containing Sepharose beads were incubated with 1 μg of substrate glutathione *S*-transferase–p53N66 (NH$_2$-terminal 66 amino acids of p53 fused to glutathione *S*-transferase) in ATM assay buffer [25 mmol/L HEPES (pH 7.4), 75 mmol/L NaCl, 3 mmol/L MgCl$_2$, 2 mmol/L MnCl$_2$, 50 μmol/L Na$_3$VO$_4$, 500 μmol/L DTT, and 5% v/v glycerol] at 37°C in the presence or absence of inhibitor. After 10 minutes with gentle shaking, ATP was added to a final concentration of 50 μmol/L and the reaction continued at 37°C for an additional 1 hour. The plate was centrifuged at 250 × g for 10 minutes (4°C) to remove the ATM-containing beads, and the supernatant was removed and transferred to a white opaque 96-well plate and incubated at room temperature for 1.5 hours to allow glutathione *S*-transferase–p53N66 binding. This plate was then washed with PBS, blotted dry, and analyzed by a standard ELISA technique with a phospho-serine 15 p53 antibody (Cell Signaling Technology, Inc., Beverly, MA). The detection of phosphorylated glutathione *S*-transferase–p53N66 substrate was performed in combination with a goat antimouse horseradish peroxidase-conjugated secondary antibody (Pierce, Rockford, IL). Enhanced chemiluminescence solution (NEN, Boston, MA) was used to produce a signal and chemiluminescent detection was carried out via a TopCount (Packard, Meriden, CT) plate reader.

ATR kinase activity was determined as for ATM except that the kinase was extracted by immunoprecipitation with antiserum raised to amino acids 400–480 of ATR (30). mTOR protein was isolated from HeLa cell cytoplasmic extract by immunoprecipitation and activity determined essentially as previously described (31) with recombinant PHAS-1 as a substrate. The DNA-PK (24, 32), PI3K (28), and PI4K (33) assays were performed essentially as described previously.

The concentration of inhibitor that achieved 50% inhibition of the enzyme (IC$_{50}$) for KU-55933 (and KU-58050 for ATM) in all assays was derived from sigmoidal plots with GraphPad Prism version 3.03 for Windows (GraphPad Software, San Diego, CA). Enzyme activity was plotted against concentration of inhibitor compound, and the data were calculated from the means of at least three independent experiments.

Kinetic Analysis. The activity of ATM was assayed using the ELISA technique described above. For inhibition experiments, KU-55933 was added to the reaction mixture and preincubated for 10 minutes before addition of ATP. Inhibition was performed at 0, 1, 5, 10, 20, or 40 nmol/L KU-55933 in varying concentrations of ATP (0.5 to 100 μmol/L). Ki was determined following standard Michaelis-Menten kinetics and with the Lineweaver Burke double reciprocal plot.

Cell-based Determinations of ATM Inhibition. U2OS cells [which have a robust p53 response (34)] were exposed to ionizing radiation (3, 5, or 15 Gy) or UV (5 or 50 J/m^2) and the ATM response determined by Western blot analysis of p53 serine 15 phosphorylation and stabilization of wild-type p53. Whole cell extracts were obtained from each time point, proteins separated by SDS-PAGE, and the ATM-specific increase in phosphorylated serine 15 measured with a p53 phospho-serine 15 specific antibody (Cell Signaling Technology, Inc.). Overall p53 stabilization with time was also observed with a p53-specific antibody (DO-1; Santa Cruz Biotechnology, Santa Cruz, CA). Similarly, for studying ATM-dependent phosphorylations on H2AX, CHK1, NBS1, and SMC1, the following antibodies were used: CHK1 phospho-serine 345 and NBS1 phospho-serine 343 antibodies were purchased from Cell Signaling Technology, Inc. Histone H2A (H-124) and CHK1 antibodies were from Santa Cruz Biotechnology. SMC1 and SMC1 phospho-serine 966 antibodies were from Bethyl Laboratories (Montgomery, TX). NBS1 antibody was from Oncogene (Cambridge, MA), and H2AX phospho-serine 139 (JBW301) was from Upstate Technology (Charlottesville, VA). For determination of a cellular IC$_{50}$ for KU-55933, the peak response time for p53 serine 15 phosphorylation of 2 hours was used to monitor inhibition of ATM. The compounds were titrated onto cells and preincubated for 1 hour before ionizing radiation. Using scanning densitometry, the percentage inhibition relative to vehicle control was calculated, and the IC$_{50}$ value was calculated as for the *in vitro* determinations.

Cytotoxicity Studies. The effect of ATM inhibition on cellular survival was measured by clonogenic assays. For HeLa cells, tissue culture treated 6-well plates were seeded at an appropriate concentration to give 100 to 200 colonies per well and returned to the incubator to allow the cells to attach. Four hours later, compound or vehicle control was added to the cells. For the standard clonogenic survival studies, the cells were incubated for 1 hour in the presence of inhibitor before irradiation or the addition of chemotherapeutic compounds. The cells were then incubated for 16 hours before the media were replaced with fresh DMEM in the absence of drugs. After 7 to 14 days (depending on cell type), colonies formed were fixed and stained with Giemsa (Sigma) and scored with a ColCount-automated colony counter (Oxford Optronics Ltd., Oxford, United Kingdom). The data were calculated as surviving fractions with respect to vehicle controls ± SE. For the analysis of the cytotoxic effects of etoposide on LoVo, SW620, V3, and V3YAC cells, the clonogenic assay was performed as described previously (32): briefly, exponentially growing cells in 6-well plates were exposed to drugs for 16 hours, harvested by trypsinization, counted, and seeded into 10-cm Petri dishes at densities varying from 100 to 100,000 cells per dish in fresh medium for colony formation. Colonies were stained with crystal violet after 7 to 14 days, counted as above and the data were normalized to vehicle controls. The sensitizer enhancement ratio was calculated as the surviving fraction of cells in the absence of KU-55933 divided by the surviving fraction of cells in the presence of KU-55933 for any given dose or concentration of cytotoxic insult.

Cell Cycle Analysis. 1BR or AT4 cells were seeded in 10-cm Petri dishes and treated on day 2 (80 to 90% confluence). Cells were preincubated for 1 hour with KU-55933 or vehicle control and then exposed to 5 Gy of ionizing radiation (Faxitron 43855D, dose rate 1 Gy/min). Time courses of cell cycle distribution were performed (data not shown), and the optimal time for discrimination of populations was selected as 16 hours. All subsequent experiments were performed at the 16-hour time point. Cells were stained with propidium iodide according to standard protocols (35) and analyzed by FACS with a FACScalibur (BD Biosciences, Franklin Lakes, NJ). Exponentially growing (50–70% confluent) SW620 cells in 60 mm dishes were exposed to KU-55933 or DMSO for 1 h before addition of etoposide (final concentration of 0.1 and 1 μmol/L) for 16 h before harvesting, propidium iodide staining and analysis as above.

9153

RESULTS

IC$_{50}$ and Kinetic Analysis of KU-55933. Through screening of a small library of molecules designed around the relatively nonspecific PIKK inhibitor LY294002 (to be described elsewhere), we identified a potent inhibitor of ATM kinase activity termed KU-55933 (Fig. 1). By analysis of concentration *versus* percentage inhibition curves, it was determined that the IC$_{50}$ for KU-55933 was 12.9 ± 0.1 nmol/L. Counterscreening this molecule against other members of the PIKK family (Table 1) demonstrated that the compound exhibited at least a 100-fold differential in selectivity. Furthermore, in screening a commercially available panel of 60 kinases (Upstate Biotechnology, Lake Placid, NY), it was found that at a single point concentration of 10 μmol/L, KU-55933 did not significantly inhibit any kinase tested (data not shown). By contrast, the related molecule KU-58050 (Fig. 1), which has a piperidine replacement to the morpholine moiety of KU-55933, had a calculated IC$_{50}$ against ATM of only 2.96 ± 0.44 μmol/L. This result highlights the importance of the morpholine oxygen for ATM inhibition. The importance of a hydrogen bond mediated between the morpholine oxygen of LY294002 and the hinge region of PI3k p110γ was highlighted in a recent crystal structure determination (36). KU-58050 thus serves as a useful negative control compound for the cellular studies described below because its IC$_{50}$ for ATM is ~230 times higher than that for KU-55933.

On the basis of the structural similarity between KU-55933 and LY294002 (24, 28), it was assumed that the inhibition of ATM by KU-55933 would be ATP competitive. Indeed, Lineweaver-Burke plots revealed a characteristic behavior of competitive inhibition (data not shown). From the slopes of the primary plots, we derived the Ki for KU-55933 as 2.2 ± 0.3 nmol/L additionally showing the potency of the compound as an ATM inhibitor.

Inhibition of ATM-dependent Cellular Phosphorylation Events. To assess the function of ATM at the cellular level, we looked at the phosphorylation status of serine 15 of p53, a marker of ATM activity (10, 11) after treating U2OS osteosarcoma cells with ionizing radiation. Western blot analysis with a phospho-serine 15 specific antibody showed that the predicted response was evident after 10 minutes and was maintained up to 4 hours after ionizing radiation induction [Fig. 2*A(i)*, top panel]. The classic stabilization of the p53 protein after ionizing radiation was also clearly observed [Fig. 2*A(i)*, bottom panel]. Strikingly, when this experiment was carried out in the presence of 10 μmol/L KU-55933, the ionizing radiation-induced p53 serine 15 phosphorylation was totally absent [Fig. 2*A(ii)*, top panel]. Notably, in this experiment, the stabilization of the wild-type p53 protein was evident after ionizing radiation treatment but with somewhat delayed kinetics compared with that observed in the control cells [Fig. 2*A(ii)*, bottom panel]. This proved that KU-55933 was active at the cellular level in ablating a well-characterized ATM-dependent phosphorylation event. By monitoring p53 serine 15 phosphorylation at the 2-hour time point after ionizing radiation, we went on to analyze effective concentrations of KU-55933 and KU-58050 required to inhibit cellular ATM function. Fig. 2*B* reveals that KU-55933 has a

Table 1 *Inhibition of kinase activity by KU-55933 for ATM and related kinases*

Enzyme	IC$_{50}$ (nmol/L)
ATM	12.9 ± 0.1
DNA-PK	2,500 ± 340
PI3K	16,600 ± 1,700
ATR	>100,000
PI4K	>100,000
mTOR	9,300 ± 420

NOTE. The IC$_{50}$ was calculated from sigmoid plots of increasing concentrations of KU-55933 *versus* activity for each of the kinases. Data represent the mean of five independent experiments ± SE.

dose-dependent effect in inhibiting this ATM-dependent phosphorylation event with an estimated IC$_{50}$ of 300 nmol/L. Furthermore, and consistent with results obtained in the enzymatic assays, the data in Fig. 2*B* show that KU-58050 does not prevent the ATM-dependent phosphorylation of p53 serine 15 until a dose of 30 μmol/L.

We then went on to study whether other characterized ATM-dependent phosphorylation targets can be inhibited by KU-55933. Moreover we also looked to see if our inhibitor affected UV-mediated DNA damage signaling; a process known not be driven predominantly by ATM. Fig. 2*C* shows that the addition of KU-55933 has no appreciable effects on UV-induced phosphorylation of H2AX on serine 139 (37), NBS1 on serine 343 (38), CHK1 on serine 345 (39), and SMC1 on serine 966 (40). In stark contrast to the UV responses, KU-55933 ablates the ionizing radiation-induced phosphorylation of these ATM substrates. Similar data (not shown) were also obtained for other ATM-mediated phosphorylation events on CHK2, MDC1, TopBP1, and BRCA1 in response to ionizing radiation but not to UV-mediated DNA damage. Taken together, these results additionally highlight the specific nature of the inhibitor and reveal that at the dose used (10 μmol/L), the molecule is highly specific at inhibiting ATM-dependent ionizing radiation-mediated DNA damage responses in living cells in line with our findings in the biochemical enzymatic assays (Table 1). These results also clearly demonstrate that KU-55933 does not appreciably inhibit the cellular activities of the most closely related enzyme to ATM, ATR, which is a known early responder to UV-induced DNA damage.

Cellular Radiosensitization by KU-55933. The effects of KU-55933 and KU-58050 on ionizing radiation-induced cytotoxicity were studied by *in vitro* clonogenic survival assays on the human tumor cell line HeLa (Fig. 3*A*) and on A-T fibroblasts (Fig. 3*B*). KU-55933 was found to maximally potentiate ionizing radiation-induced cell killing at a concentration of 10 μmol/L and was hence used at this dose in these and later experiments (data not shown). Note, that at a concentration of 1 μmol/L the sensitizer enhancement ratio at 2 Gy was 1.8 on HeLa cells (data not shown). It should be noted that neither of the two compounds alone, at concentrations up to 10 μmol/L, were found to significantly reduce the clonogenic survival of the cell lines tested. Fig. 3*A* clearly reveals that KU-55933 sensitizes HeLa cells to a range of ionizing radiation doses whereas KU-58050 does not. In the case of HeLa cells, the sensitizer enhancement ratio at 2 Gy, for 10 μmol/L of KU-55933 was 2.6 ± 0.6. Similar data has been obtained with the LoVo and SW620 cell lines (data not shown). Highlighting the specific nature of ATM inhibition, we found that A-T fibroblasts were not sensitized to the effects of KU-55933 in combination with ionizing radiation (Fig. 3*B*). This is consistent with KU-55933 specifically inhibiting ATM but not the other DNA damage-activated PIKKs, ATR, and DNA-PK (Table 1).

Cellular Chemosensitization by KU-55933. As well as their hypersensitivity toward ionizing radiation, A-T cells have also been shown to be sensitive to other DNA-damaging agents such as the topoisomerase I and II poisons (41–43). In contrast, DNA-damaging agents that do not effectively yield DNA double-strand breaks such as
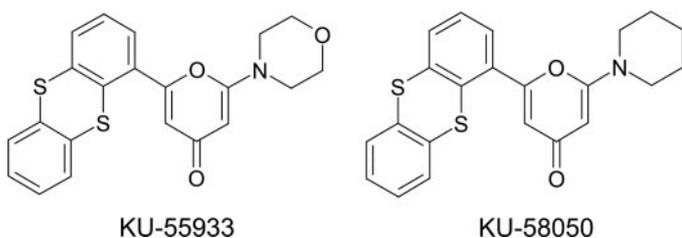

Fig. 1. Chemical structures of morpholin-4-yl-6-thianthren-1-yl-pyran-4-one (KU-55933) and 2-piperidin-1-yl-6-thianthren-1-yl-pyran-4-one (KU-58050).
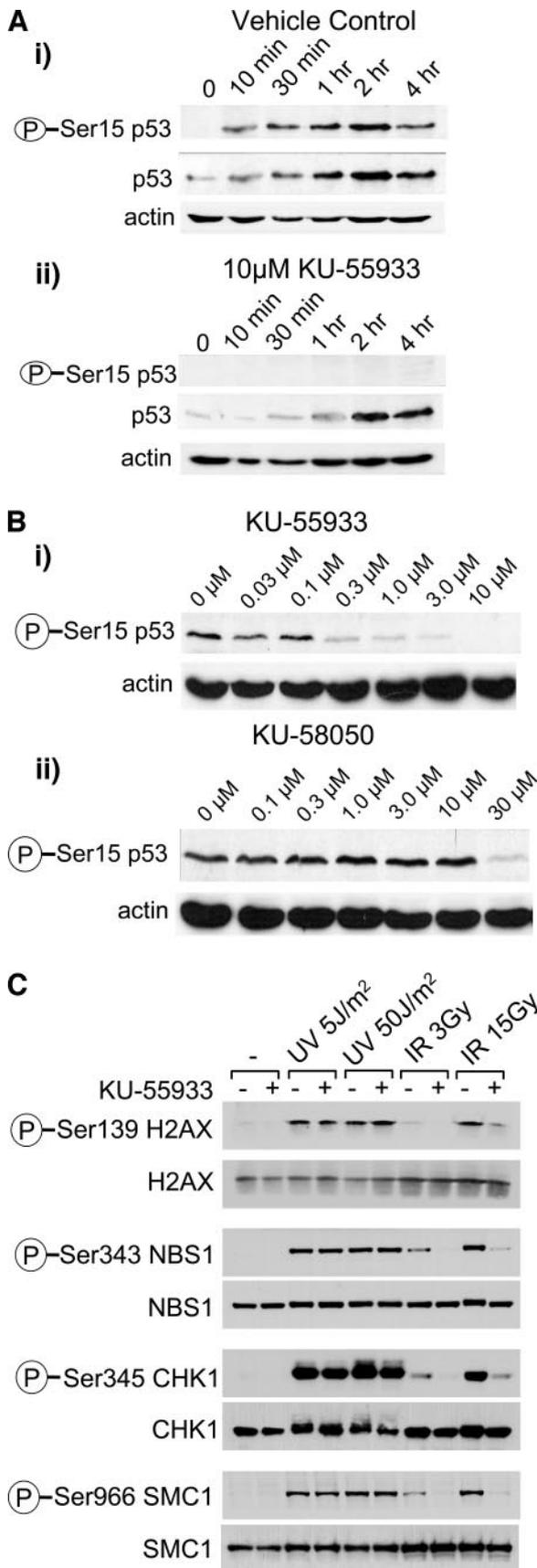
9154

Fig. 2. Effect of KU-55933 and KU-58050 on p53 serine 15 phosphorylation and total p53 protein levels in response to ionizing radiation (IR) and their effects on ATM substrates after UV or IR treatment. *A.* Exposure of U2OS cells to 5 Gy of IR was followed by incubation at 37°C, for the time points shown, to monitor p53 phospho-serine 15 or total p53 levels by Western blot analysis. Protein loading levels were monitored by
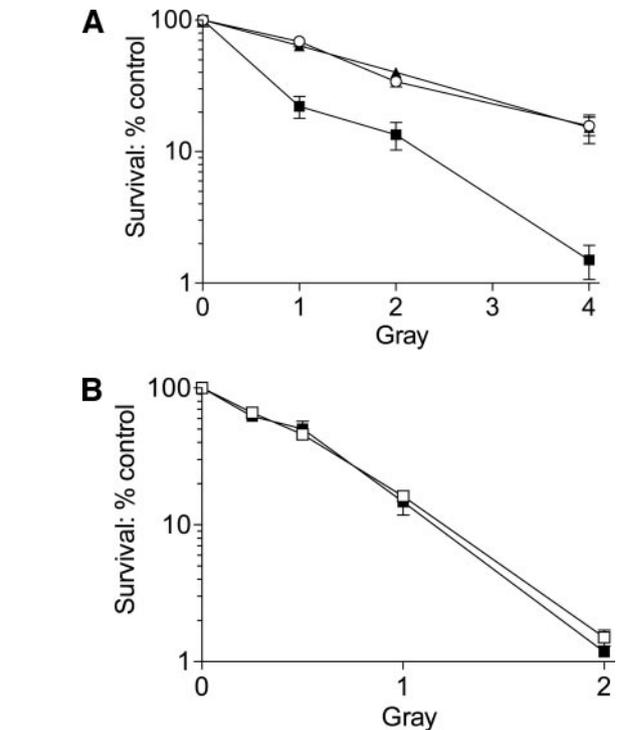

Fig. 3. Effect of KU-55933 and KU-58050 on cellular survival of HeLa and A-T fibroblasts in response to ionizing radiation. *A.* HeLa cells were treated for 1 hour with either vehicle (○), 10 μmol/L KU-55933 (■), or 10 μmol/L KU-58050 (▲) before irradiation, then allowed to grow for 16 hours before media replacement and colony formation. *B.* AT4 fibroblasts were treated for 1 hour with vehicle or 10 μmol/L KU-55933 before irradiation and allowed to grow for 16 hours before media replacement and colony formation; AT4 cells in the presence (■) or absence (□) of 10 μmol/L KU-55933. Data are the mean of at least three independent experiments ± SE.

alkylating agents, intra- or interstrand cross-linkers, do not preferentially kill A-T cells. To study if the effects of ATM inhibition mirrored the aforementioned effects seen by cells lacking the ATM protein, we exposed cells to a variety of chemotherapeutic agents in the presence or absence of KU-55933 (Fig. 4). Through clonogenic survival assays we found that KU-55933 sensitizes HeLa cells to the cytotoxic effects of the topoisomerase II inhibitors etoposide, doxorubicin, amsacrine (Fig. 4*A*–*C*), and the topoisomerase I inhibitor camptothecin (Fig. 4*D*). The negative control molecule KU-58050 had no impact on cellular survival in response to either etoposide (Fig. 4*A*) or camptothecin (Fig. 4*D*), again highlighting the specific nature of KU-55933. To additionally investigate the sensitization of cells to the cytotoxic effects of etoposide by KU-55933, equipotent doses of etoposide were administered to LoVo (1 μmol/L) and SW620 (1 μmol/L) cells, as well as to the DNA-dependent protein kinase catalytic subunit (DNA-PKcs) −/− V3 (0.3 μmol/L) and the DNA-PKcs complemented derivative V3-YAC (1 μmol/L) cells (Table 2). The DNA-PKcs–deficient V3 line was greatly sensitized by the ATM inhibitor, thus indicating the cumulative effects of the loss of a key DNA damage

probing for actin. The experiment was conducted (*i*) in the absence or (*ii*) the presence of 10 μmol/L KU-55933. *B.* Cellular IC_{50} determination of ATM inhibition by (*i*) KU-55933 or (*ii*) KU-58050. U2OS cells were preincubated in varying concentrations of compound as shown for 1 hour before 5 Gy of irradiation. After 2 hours, the cells were analyzed for p53 phospho-serine 15 levels by Western blotting. Protein loading was monitored for by actin levels as shown. All images are representative data of experiments performed $n = 3$. *C.* Effect of KU-55933 on a range of ATM target phosphorylation events in response to UV (5, 50 J/m²) or IR (3, 15Gy) in U2OS cells. U2OS cells were pretreated for 1 hour with 10 μmol/L KU-55933 before irradiation as shown. After 2 hours, total cellular extracts were analyzed for H2AX phospho-serine 139, NBS1 phospho-serine 343, CHK1 phospho-serine 345, or SMC1 phospho-serine 966. Levels of the respective native proteins are shown as a control for equal protein loading.
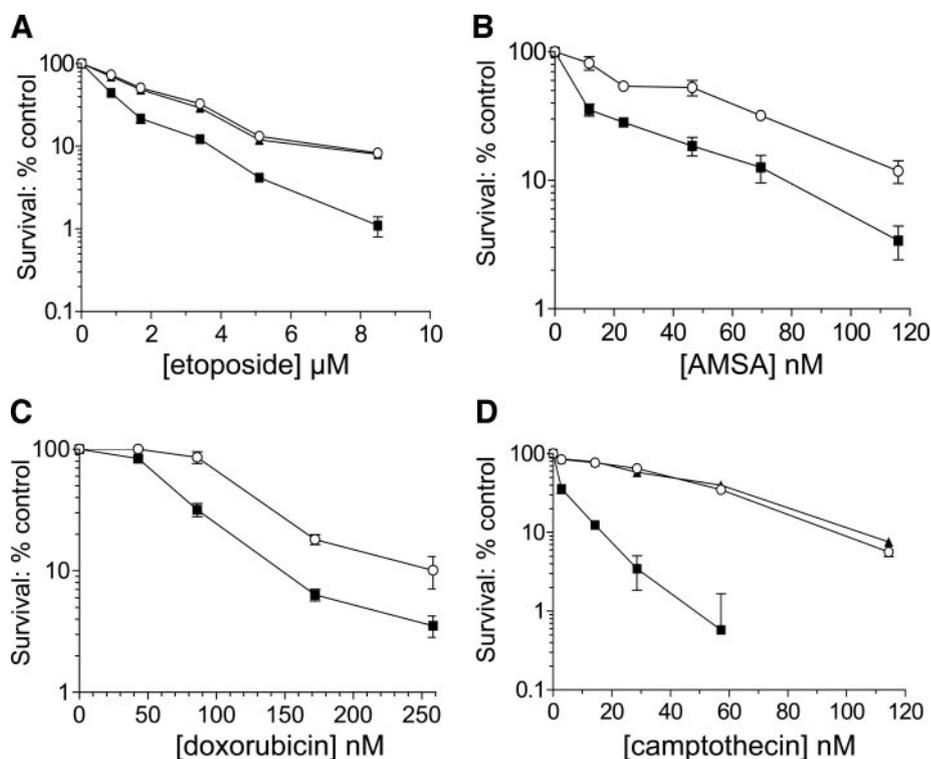
9155

Fig. 4. Potentiation of topoisomerase poison induced killing by KU-55933 but not KU-58050. HeLa cells were exposed to increasing doses of cytotoxic agent after 1 hour of preincubation with vehicle (○), 10 μmol/L KU-55933 (■), or 10 μmol/L KU-58050 (▲) for 16 hours before media replacement and colony formation. A, etoposide; B, amsacrine (AMSA); C, doxorubicin; or D, camptothecin. Data are the mean of at least three independent experiments ± SE.

signaling protein and a key component of a major DNA double-strand break repair pathway, nonhomologous end joining.

In stark contrast to the effects of KU-55933 on DNA double-strand break-inducing agents, the molecule was found not to sensitize HeLa cells to the cytotoxic effects of the alkylating and cross-linking agents cisplatin and melphalan, the interstrand cross-linking agent mitomycin C, and the alkylating agent chlorambucil (data not shown). Similar results were also seen when LoVo cells were used (data not shown).

Effects of KU-55933 on the Cell Cycle. One of the hallmarks of A-T cells is their inability to mediate the G_1-S–, intra-S–, and G_2-M– phase DNA damage checkpoints in response to ionizing radiation (7, 9). Ultimately, in response to DNA double-strand breaks, A-T cells will arrest at the G_2 stage of the cell cycle (9). To study the effects of ATM inhibition via KU-55933 on cell cycle distribution, we have analyzed asynchronous cells pre- and postexposure to 5 Gy of ionizing radiation or to etoposide. There is no effect on the cell cycle distributions from exposure to KU-55933 alone (Fig. 5A–C). After exposure to ionizing radiation, the distribution of the cells shifts, as shown in Fig. 5A. For 1BR cells, this shift is manifest as clear G_1 and G_2 peaks in the absence of KU-55933, consistent with the cells accumulating at the G_1-S and G_2-M checkpoints in response to ionizing radiation induced DNA damage. In the presence of KU-55933 however, these responses of 1BR cells are significantly altered (Fig. 5A), with the distribution showing a large accumulation of cells in G_2-M. The cell cycle distribution of SW620 cells after exposure to etoposide was also affected by KU-55933 (Fig. 5C), again with a significant increase in the G_2-M population. These data are therefore consistent with KU-55933 preventing the normal ATM-dependent cell cycle checkpoint responses to ionizing radiation, leading to the eventual activation of an ATM-independent arrest at the G_2-M stage.

To demonstrate the specificity of KU-55933 in regards to the above effects, we also studied its effects on cell cycle distribution in A-T fibroblasts. As shown in Fig. 5B, the cell cycle distribution of the AT4 cells was altered after exposure to ionizing radiation with the cells arresting predominantly in G_2, consistent with published data for an asynchronous population of A-T cells (9). Significantly, this response to ionizing radiation was not altered in the presence of KU-55933 (Fig. 5B), revealing that the effects of the molecule on cell cycle distribution after ionizing radiation are ATM dependent.

DISCUSSION

Small molecule inhibitors of enzymes or receptors may not only ultimately lead to the development of therapeutics but are also useful probes for elucidating the mechanisms of action and function of proteins and pathways. The PIKK family of protein kinases, of which ATM is a member, has been studied at the cellular and molecular levels by a variety of means, including employment of small molecule inhibitors such as caffeine, wortmannin, and LY294002 (23, 24, 26–28). However, interpretation of results obtained with these molecules has been made difficult by concerns over their specificity and mechanism of action. Here, we have described the characterization of a novel and specific inhibitor of the ATM kinase termed KU-55933. This molecule has an IC_{50} of 12.9 nmol/L against the native enzyme and exhibits an ATP competitive mechanism of action. Importantly, this potency is essentially restricted to ATM as it is at least 100-fold more potent against ATM than against the other PIKK family mem-

Table 2 *Survival of cell lines exposed to etoposide in the presence or absence of KU-55933*

	Survival (%)		Sensitizer enhancement ratio
	0 μmol/L KU-55933	10 μmol/L KU-55933	
LoVo	24.5 ± 0.28	5.8 ± 0.3	4.2
SW620	43.9 ± 0.1	2.3 ± 0.6	19.3
V3	24.5 ± 3.8	0.7 ± 0.4	36.5
V3YAC	32.4 ± 1.3	1.8 ± 0.3	17.8

NOTE. Cells were preincubated with DMSO or KU-55933 for 1 hour before exposure to etoposide +/− KU-55933 for an additional 16 hours. Data are survival in the absence or presence of KU-55933 for approximately equipotent concentrations of etoposide (0.3 μmol/L for V3 and 1 μmol/L for LoVo, SW620, and V3YAC) ± SE (n = 3) normalized to DMSO control.
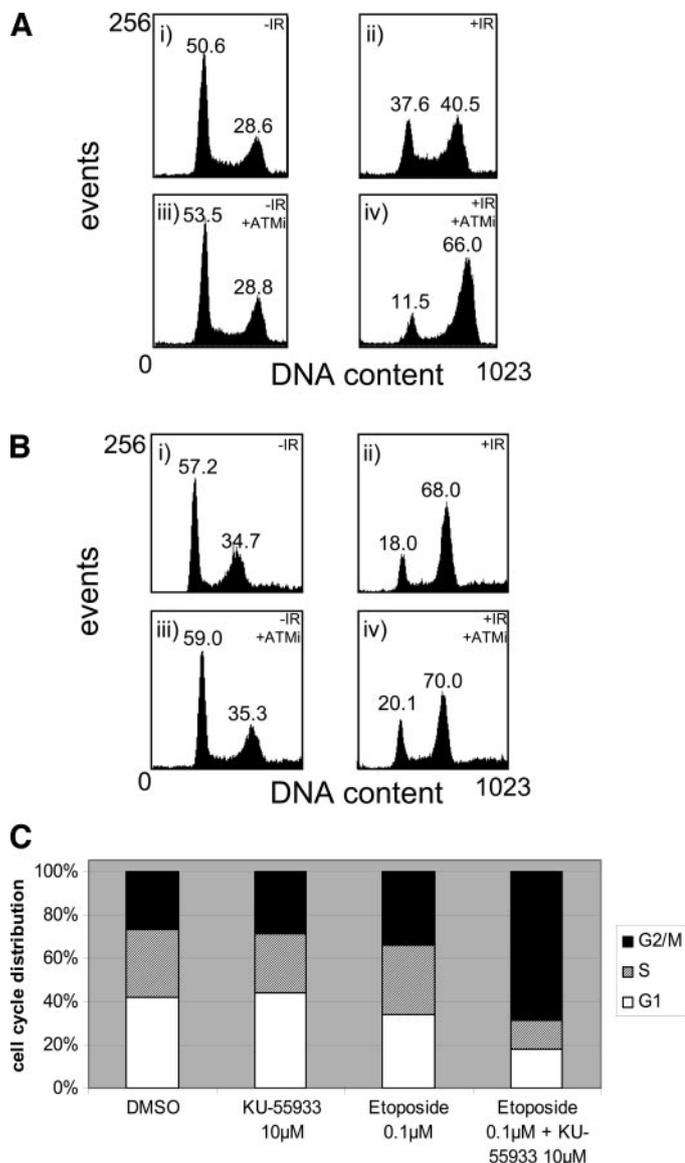
9156

Fig. 5. Cell cycle analysis: perturbation of ionizing radiation (IR)- and etoposide-induced cell cycle profiles by KU-55933. *A*. Asynchronous 1BR cells were preincubated in DMSO (*i* and *ii*), or 10 μmol/L KU-55933 ATM inhibitor (ATMi) (*iii* and *iv*) and mock irradiated (*i* and *iii*), or irradiated (5Gy of IR; *ii* and *iv*). Sixteen hours later, the cells were harvested and fixed before staining with propidium iodide and analysis by flow cytometry. Red fluorescence intensity was measured and histograms of DNA content generated. The cell cycle profiles of individual experiments are presented for display purposes. The numbers in the panels are the proportion of cells present at G_1 and G_2-M as determined in three independent experiments ± SE. *B*, as in *A*, except with AT4 cells. *C*. The cell cycle distribution after exposure to etoposide in SW620 cells was determined and the data plotted in the bar chart (G_1, □; S, ▨; and G_2-M, ■).

bers tested and shows no activity against a panel of 60 unrelated kinases. Of key importance here was that the closest family member with regards to homology across the ATP-binding domain, ATR, was not inhibited at doses up to 100 μmol/L. By way of comparison, wortmannin only exhibits ~10 fold more potency against ATM in comparison to ATR (23) and hence can be ineffectual in studies where discrimination between these related DNA damage-activated kinases is required.

As an initial study to understand the key attributes for the binding of KU-55933 to the ATP active site of ATM, we produced the molecule KU-58050. Similar in all respects to KU-55933 other than an oxygen in the cyclic amine side chain, KU-58050 was in comparison a very poor ATM inhibitor with an IC_{50} > 200 times than that

seen for KU-55933. The chemical substitution of replacing the morpholine group with a piperidine highlights the importance of the morpholine oxygen. On the basis of the crystal structure of the porcine PI3K p110γ subunit in complex with LY294002 (36), the morpholine is most probably hydrogen bonding within the hinge region of the ATP-binding site of ATM. This of course can only be fully established from a crystal structure determination of ATM bound with KU-55933. Additional structure-activity relationships surrounding KU-55933 are taking place at present to give a better understanding about other key features of the molecule required for its strong potency and selectivity toward ATM. Although a weakly active molecule against ATM, KU-58050 acts as a useful control molecule to study the specificity of KU-55933 as described in the work presented here.

The role of the ATM protein in the stabilization of p53 in response to DNA double-strand break-inducing agents is very well established (4, 10, 11, 13, 44). The direct phosphorylation of p53 on serine 15 by ATM is a key early event in this process (10, 11). We have shown that KU-55933 prevents this cellular phosphorylation event in a concentration-dependent manner. Interestingly, in the U2OS cell line we have studied, the stabilization of p53 still occurs in the presence of KU-55933, albeit in a delayed fashion. This is similar to the suboptimal induction of p53 seen in some A-T cell lines (44). It has been speculated that the eventual induction of p53 in such A-T cells occurs by the back-up or partially redundant action of ATR in phosphorylating p53 on serine 15 in the absence of ATM (3, 4, 30). Notably, however, we did not see any serine 15 phosphorylation after ionizing radiation in the presence of KU-55933 suggesting that, over the time course of this experiment, ATR is not activated to a significant degree and that some other mechanism(s) is involved in the gross stabilization of p53. Another key phosphorylation event on p53, which is believed to be involved in disrupting the p53/Mdm2 interaction, leading to p53 stabilization, is on serine 20 (45). This phosphorylation is thought to be mediated by the downstream target of ATM, CHK2. Consistent with KU-55933 efficiently preventing ATM activation, we have also been unable to see serine 20 phosphorylation of p53 in response to ionizing radiation in cells treated with the drug (data not shown).

A number of other substrates for ATM have been discovered and similar to p53, these have generally been found to also be cellular substrates for ATR in response to UV irradiation (3, 4). We have shown quite clearly that for a range of these substrates that we have tested (*e.g.,* SMC-1, NBS-1, and CHK-1) in response to the ionizing radiation treatment of cells, KU-55933 almost completely ablates these phosphorylation events. Notably, however, is that the phosphorylation of H2AX on serine 139 is not completely inhibited by KU-55933 in response to ionizing radiation. This most probably reflects the fact that this site is also targeted by DNA-PK after ionizing radiation (46). As one would expect from the *in vitro*-specific nature of KU-55933, the molecule did not prevent UV phosphorylation events on the proteins we studied, most probably reflecting the fact that the agent does not inhibit these ATR-dependent events. Through the use of KU-55933, it will be intriguing to study other ATM-dependent sites of phosphorylation, in particular, the serine 1981 autophosphorylation site (47)

A classic hallmark of cells derived from A-T patients is their extreme sensitivity to ionizing radiation (5, 19, 21). We have shown that KU-55933 can recapitulate this phenotype in a range of cell lines and that it does not additionally sensitize A-T cells to the effects of ionizing radiation. By contrast, we were able to additionally sensitize DNA-PKcs–deficient cells to the effects of etoposide indicating the distinct nature of the ATM and DNA-PK pathways in response to DNA double-strand breaks. As it has been shown that certain cell

9157

types derived from A-T mice are not hypersensitive to ionizing radiation (48), it will be interesting to evaluate the radiosensitizing effects of KU-55933 on a range of different cell types and tissues. For the ultimate development of a clinical radiosensitizor, the effects of ATM inhibition on normal tissues must also be evaluated and understood. KU-55933 will be a useful tool to address this key issue.

Hypersensitivity to DNA double-strand break-inducing agents is a characteristic of ATM-deficient cells (5). In this study, we have shown that KU-55933 can sensitize ATM-proficient cells to DNA double-strand break-inducing agents other than ionizing radiation. The topoisomerase I inhibitor camptothecin, although initially producing a DNA single-strand break, ultimately produces a DNA double-strand break during replication, which is presumed to be the lethal lesion (49). KU-55933 sensitized cells to camptothecin, consistent with the known sensitivity of A-T cells to this particular agent (50). Similarly, the topoisomerase II inhibitors used had their lethal effects (51) enhanced in the presence of the ATM inhibitor. Again, this is in keeping with observations with cells defective in ATM (41–43). One might have expected some differences between the phenotypes of A-T cells and ATM-inhibited cells because inhibited ATM could act in a dominant-negative fashion, whereas in A-T cells, the protein is generally not present. However in these initial studies, we did not observe anything strikingly different between the two scenarios. Finally, and in line with the fact that A-T cells are not markedly hypersensitive to DNA-alkylating agents or interstrand cross-linking agents (5, 43, 52, 53), we found that KU-55933 did not sensitize cells to such drugs.

ATM-deficient cells are well known as being defective in the major cell cycle checkpoints after DNA damage (4–9). Therefore, it would be expected that the addition of an ATM inhibitor to ATM-proficient cells would yield a similar phenotype. Indeed, we found that KU-55933 perturbed the checkpoint effects of 1BR cells in response to ionizing radiation and SW620 cells in response to etoposide, producing a similar shift in cell cycle distribution to that seen in irradiated A-T cells. Moreover, the molecule did not affect the ionizing radiation-induced cell cycle profile of A-T cells in response to ionizing radiation, once again highlighting the highly specific actions of this molecule. Clearly, additional studies to monitor the effects of KU-55933 at specific checkpoints are warranted.

The discovery and characterization of KU-55933 as a specific and cellularly active ATM inhibitor raises the exciting prospect that derivatives of this molecule may serve as novel radio- and chemosensitizors in clinical settings. Recent reports have highlighted the use of antisense or small interfering RNAs to deplete ATM function in human tumor cells as a means of radiosensitization (54–57). To our knowledge, however, our work is the first to evaluate a small molecule approach to target ATM. Taken together, with data obtained through other approaches, our results reinforce the view that the ATM protein kinase represents a tractable and highly attractive target for the development of novel types of anticancer agent.

ACKNOWLEDGMENTS

REFERENCES

1. Rouse J, Jackson SP. Interfaces between the detection, signaling and repair of DNA damage. Science (Wash. DC) 2002;297:547–51.
2. Zakian VA. ATM-related genes: what do they tell us about functions of the human gene? Cell 1995;82:685–7.
3. Abraham RT. Cell cycle checkpoint signaling through the ATM and ATR kinases. Genes Dev 2001;15:2177–96.
4. Shiloh Y. ATM and related protein kinases: safeguarding genome integrity. Nat Cancer Rev 2003;3:155–68.
5. Lavin MF, Shiloh Y. The genetic defect in ataxia-telangiectasia. Annu Rev Immunol 1997;15:177–202.
6. Rotman G, Shiloh Y. ATM. from gene to function. Hum Mol Genet 1988;7:1555–63.
7. Kastan MB, Lim DS. The many substrates and functions of ATM. Nat Rev Mol Cell Biol 2000;1:179–86.
8. Shiloh Y. ATM and ATR: networking cellular responses to DNA damage. Curr Opin Genet Dev 2001;11:71–7.
9. Xu B, Kim ST, Lim DS, Kastan MB. Two molecularly distinct G_2-M checkpoints are induced by ionizing irradiation. Mol Cell Biol 2002;22:1049–59.
10. Canman CE, Lim DS, Cimprich KA, et al. Activation of the ATM kinase by ionizing radiation and phosphorylation of p53. Science (Wash. DC) 1988;281:1677–9.
11. Banin S, Moyal L, Shieh S, et al. Enhanced phosphorylation of p53 by ATM in response to DNA damage. Science (Wash. DC) 1998;281:1674–7.
12. Matsuoka S, Rotman G, Ogawa A, Shiloh Y, Tamai K, Elledge SJ. Ataxia telangiectasia-mutated phosphorylates Chk2 in vivo and in vitro. Proc Natl Acad Sci 2000;97:10389–94.
13. Maya R, Balass M, Kim ST, et al. ATM-dependent phosphorylation of Mdm2 on serine 395: role in p53 activation by DNA damage. Genes Dev 1999;15:1067–77.
14. Zhao S, Weng YC, Yuan SS, et al. Functional link between ataxia-telangiectasia and Nijmegen breakage syndrome gene products. Nature (Lond.) 2000;405:473–7.
15. Bao S, Tibbetts RS, Brumbaugh KM, et al. ATR/ATM-mediated phosphorylation of human Rad17 is required for genotoxic stress responses. Nature (Lond.) 2001;411:969–74.
16. Xu B, Kim ST, Kastan MB. Involvement of Brca1 in S-phase and G_2-phase checkpoints after ionizing irradiation. Mol Cell Biol 2001;21:3445–50.
17. Fornace AL Jr, Little JB. Normal repair of DNA single-strand breaks in patients with ataxia-telangiectasia. Biochem Biophys Acta 1980;607:432–7.
18. Lavin MF, Davidson M. Repair of strand breaks in superhelical DNA of ataxia-telangiectasia lymphoblastoid cells. J Cell Sci 1981;48:383–91.
19. Cornforth MN, Bedford JS. On the nature of a defect in cells from individuals with ataxia-telangiectasia. Science (Wash. DC) 1985;227:1589–91.
20. Coquerelle TM, Weibezahn KF, Lucke-Huhle C. Rejoining of double strand breaks in normal human and ataxia-telangiectasia fibroblasts after exposure to ^{60}Co gamma-rays, ^{241}Am alpha-particles or bleomycin. Int J Radiat Biol Relat Stud Phys Chem Med 1987;51:209–18.
21. Foray N, Priestley A, Alsbeih G, et al. Hypersensitivity of ataxia-telangiectasia fibroblasts to ionizing radiation is associated with a repair deficiency of DNA double-strand breaks. Int J Radiat Biol 1997;72:271–83.
22. Sarkaria JN, Eshleman JS. ATM as a target for novel radiosensitizers. Semin Radiat Oncol 2001;11:316–27.
23. Sarkaria JN, Tibbetts RS, Busby EC, Kennedy AP, Hill DE, Abraham RT. Inhibition of phosphoinositide 3-kinase related kinases by the radiosensitizing agent wortmannin. Cancer Res 1998;58:4375–82.
24. Izzard RA, Jackson SP, Smith GCM. Competitive and non-competitive inhibition of the DNA dependent protein kinase. Cancer Res 1999;59:2581–6.
25. Ui M, Okada T, Hazeki K, Hazeki O. Wortmannin as a unique probe for an intracellular signalling protein, phosphoinositide 3-kinase. Trends Biochem Sci 1995;20:303–7.
26. Zhou B-B S, Chaturvedi P, Spring K, et al. Caffeine abolishes the mammalian G_2-M DNA damage checkpoint by inhibiting ataxia-telangiectasia–mutated kinase activity. J Biol Chem 2000;5:10342–8.
27. Block WD, Merkle D, Meek K, Lees-Miller SP. Selective inhibition of the DNA-dependent protein kinase (DNA-PK) by the radiosensitizing agent caffeine. Nucleic Acid Res 2004;32:1967–72.
28. Vlahos CJ, Matter WF, Hui KY, Brown RF. A specific inhibitor of phosphatidylinositol 3-kinase, 2-(4-morpholinyl)-8-phenyl-4H-1-benzopyran-4-one (LY294002). J Biol Chem 1994;269:5241–8.
29. Blunt T, Finnie NJ, Taccioli GE, et al. Defective DNA-dependent protein kinase activity is linked to V(D)J recombination and DNA repair defects associated with the murine scid mutation. Cell 1995;80:813–23.
30. Tibbetts RS, Brumbaugh KM, Williams JM, et al. A role for ATR in the DNA damage-induced phosphorylation of p53. Genes Dev 1999;13:152–7.
31. Brunn GJ, Williams J, Sabers C, Wiederrecht G, Lawrence JC, Abraham RT. Direct inhibition of the signaling functions of the mammalian target of rapamycin by the phosphoinositide 3-kinase inhibitors, wortmannin and LY294002. EMBO J 1996;15:5256–67.
32. Veuger SJ, Curtin NJ, Richardson CJ, Smith GCM, Durkacz BW. Radiosensitization and DNA repair inhibition by the combined use of novel inhibitors of DNA-dependent protein kinase and poly (ADP-ribose) polymerase-1. Cancer Res 2003;63:6008–15.
33. Zhao X-H, Bondeva T, Balla T. Characterization of recombinant phosphatidylinositol 4-kinase beta reveals auto- and heterophosphorylation of the enzyme. J Biol Chem 2000;275:14642–8.
34. Allan LA, Fried M. p53-dependent apoptosis or growth arrest induced by different forms of radiation in U2OS cells: p21WAF1/CIP1 repression in UV induced apoptosis. Oncogene 1999;18:5403–12.
35. Ormerod MG. Analysis of DNA-general methods. In: Ormerod MG, editor. Flow cytometry. Oxford, UK: Oxford University Press; 2000. p. 83–97.
36. Walker EH, Pacold ME, Perisic O, et al. Structural determinants of phosphoinositide 3-kinase inhibition by wortmannin, LY294002, quercetin, myricetin, and staurosporine. Mol Cell 2000;6:909–19.
37. Burma S, Chen BP, Murphy M, Kurimasa A, Chen DJ. ATM phosphorylates histone H2AX in response to DNA double-strand breaks. J Biol Chem 2001;276:42462–7.

38. Lim DS, Kim ST, Xu B, et al. ATM phosphorylates p95/nbs1 in an S-phase checkpoint pathway. Nature (Lond.) 2000;404:613–7.
39. Liu Q, Guntuku S, Cui XS, et al. Chk1 is an essential kinase that is regulated by Atr and required for the G_2-M DNA damage checkpoint. Genes Dev 2000;14:1448–59.
40. Kim ST, Xu B, Kastan MB. Involvement of the cohesin protein, Smc1, in Atm-dependent and independent responses to DNA damage. Genes Dev 2002;16:560–70.
41. Caporossi D, Porfirio B, Nicoletti B, et al. Hypersensitivity of lymphoblastoid lines derived from ataxia-telangiectasia patients to the induction of chromosomal aberrations by etoposide (VP-16). Mutat Res 1993;290:265–72.
42. Henner WD, Blazka ME. Hypersensitivity of cultured ataxia-telangiectasia cells to etoposide. J Natl Cancer Inst (Bethesda) 1986;76:1007–11.
43. Fedier A, Schlamminger M, Schwarz VA, Haller U, Howell SB, Fink D. Loss of atm sensitises p53-deficient cells to topoisomerase poisons and antimetabolites. Ann Oncol 2003;14:938–45.
44. Canman CE, Wolff AC, Chen C-Y, Fornace AJ Jr, Kastan MB. The p53-dependent G_1 cell cycle checkpoint pathway and ataxia-telangiectasia. Cancer Res 1994;54:5054–8.
45. Chehab NH, Malikzay A, Stavridi ES, Halazonetis TD. Phosphorylation of Ser-20 mediates stabilization of human p53 in response to DNA damage. Proc Natl Acad Sci USA 1999;96:13777–82.
46. Stiff T, O'Driscoll M, Rief N, Iwabuchi K, Lobrich M, Jeggo PA. ATM and DNA-PK function redundantly to phosphorylate H2AX after exposure to ionizing radiation. Cancer Res 2004;64:2390–6.
47. Bakkenist CJ, Kastan MB. DNA damage activates ATM through intermolecular autophosphorylation and dimer dissociation. Nature (Lond.) 2003;421:499–506.
48. Gosink EC, Chong MJ, McKinnon PJ. Ataxia-telangiectasia mutated deficiency affects astrocyte growth but not radiosensitivity. Cancer Res 1999;59:5294–8.
49. Takimoto CH, Arbuck SG. Topoisomerase I targeting agents: the camptothecins. In: Chabner BA, Longo DL, editors. Cancer chemotherapy and biotherapy: principles and practice. Philadelphia: Lippincott, Williams and Wilkins; 2001. p. 579–646.
50. Smith PJ, Makinson TA, Watson JV. Enhanced sensitivity to camptothecin in ataxia-telangiectasia cells and its relationship with the expression of DNA topoisomerase I. Int J Radiat Biol 1989;55:217–31.
51. Pommier YG, Goldwasser F and Strumberg D. Topoisomerase II inhibitors: epipodophyllotoxins, acridines, ellipticines, and bisdioxopiperazines. In: Chabner BA, Longo DL, editors. Cancer chemotherapy and biotherapy: principles and practice. Philadelphia: Lippincott, Williams & Wilkins; 2001. p. 538–78.
52. Shiloh Y, Becker Y. Kinetics of O^6-methylguanine repair in human normal and ataxia-telangiectasia cell lines and correlation of repair capacity with cellular sensitivity to methylating agents. Cancer Res 1981;41:5114–20.
53. Jaspers NG, de Wit J, Regulski MR, Bootsma D. Abnormal regulation of DNA replication and increased lethality in ataxia-telangiectasia cells exposed to carcinogenic agents. Cancer Res 1982;42:335–41.
54. Zhang N, Chen P, Gatei M, Scott S, Khanna KK, Lavin MF. An anti-sense construct of full-length ATM cDNA imposes a radiosensitive phenotype on normal cells. Oncogene 1998;17:811–8.
55. Uhrhammer N, Fritz E, Boyden L, Meyn MS. Human fibroblasts transfected with an ATM antisense vector respond abnormally to ionizing radiation. Int J Mol Med 1999;4:43–7.
56. Guha C, Guha U, Tribius S, et al. Antisense ATM gene therapy: a strategy to increase the radiosensitivity of human tumors. Gene Ther 2000;7:852–8.
57. Collis SJ, Swartz MJ, Nelson WG, DeWeese TL. Enhanced radiation and chemotherapy-mediated cell killing of human cancer cells by small inhibitory RNA silencing of DNA repair factors. Cancer Res 2003;63:1550–4.

Identification and Characterization of a Novel and Specific Inhibitor of the Ataxia-Telangiectasia Mutated Kinase ATM

Ian Hickson, Yan Zhao, Caroline J. Richardson, et al.

Updated version	Access the most recent version of this article at: http://cancerres.aacrjournals.org/content/64/24/9152

Cited articles	This article cites 48 articles, 24 of which you can access for free at: http://cancerres.aacrjournals.org/content/64/24/9152.full#ref-list-1
Citing articles	This article has been cited by 100 HighWire-hosted articles. Access the articles at: http://cancerres.aacrjournals.org/content/64/24/9152.full#related-urls

E-mail alerts	Sign up to receive free email-alerts related to this article or journal.
Reprints and Subscriptions	To order reprints of this article or to subscribe to the journal, contact the AACR Publications Department at pubs@aacr.org.
Permissions	To request permission to re-use all or part of this article, use this link http://cancerres.aacrjournals.org/content/64/24/9152. Click on "Request Permissions" which will take you to the Copyright Clearance Center's (CCC) Rightslink site.